Available online at www.sciencedirect.com
ScienceDirect
Deep-Sea Research II 55 (2008) 45–58
DEEP-SEA RESEARCH PART II
www.elsevier.com/locate/dsr2

Distribution, identity, and possible processes sustaining meso- and bathypelagic scattering layers on the northern Mid-Atlantic Ridge

A.F. Opdal[a,b,*], O.R. Godø[b], O.A. Bergstad[c], Ø. Fiksen[a]

[a]*Department of Biology, University of Bergen, Høyteknologisenteret, Pb 7800, N-5020 Bergen, Norway*
[b]*Institute of Marine Research, Pb 1870 Nordnes, N-5817 Bergen, Norway*
[c]*Institute of Marine Research, Flødevigen, N-4817 His, Norway*

Accepted 9 September 2007
Available online 28 November 2007

Abstract

As an element of comprehensive exploratory studies of the poorly known pelagic ecosystem associated with the Mid-Atlantic Ridge, acoustic data collected by R.V. *G.O. Sars* during the MAR-ECO expedition in June–July 2004 were used to describe vertical and geographical distributions of meso- and bathypelagic scattering layers. Scattering layers were observed in the entire study area and at all depths to 3000 m with a split-beam echosounder using the 18-kHz drop-keel mounted transducer. The spatial variation in density of surface to 1500 m area backscattering strength, and that of individually identifiable vertical layers, is described in relation to bathymetry and large-scale hydrographical features such as the Sub-polar Front. The inhabitants of scattering layers were identified by exploratory midwater trawling. A major pattern was the elevated backscattering associated with waters around the Charlie-Gibbs Fracture Zone (CGFZ) and the associated Sub-polar Front at and south of 52°N. In this section of the Mid-Atlantic Ridge, the interaction between topographical features, circulation and primary production appears to create favorable conditions for many taxa across all trophic levels. By comparison, the density was lower both to the south of the CGFZ towards the Azores and in particular northwards towards Iceland. Along the north–south gradient a peak in near-surface algal biomass was also found near the CGFZ, with lower values further north and south. We hypothesize that fish productivity is bottom-up regulated, i.e., limited by primary production within the ridge-associated system, supplemented by advection of allochthonous material, especially in the south.

Keywords: Mid-ocean ridge; Deep scattering layers (DSLs); Mesopelagic; Bathypelagic

1. Introduction

The around 60,000-km-long system of mid-ocean ridges spans the oceans, constituting one of the major but least explored topographical features of the planet. Pelagic biota of the oceans, including the taxa undertaking extensive vertical migrations on a daily, seasonal or ontogenetic scale, are likely to be affected by this topographical feature, which is known to affect their habitat characteristics such as currents and production patterns. In view of this potential significance, surprisingly few studies have focused on pelagic communities associated with mid-ocean ridges. Studies at seamounts and continental slopes may be relevant as references, but ridges are fundamentally different from both the isolated seamounts surrounded by deep ocean and from continental slopes where effects of coastal processes are pronounced. In contrast, mid-ocean ridges consist of connected deep valleys and shallow hills and islands, similar to mountain chains on land. As spectacular as the hills are the deep fractures and the central rift valleys associated with the ridges, some reaching almost full abyssal depths.

Open-ocean deep scattering layers (DSLs) at mesopelagic depths have been known for a long time, as has the existence of, e.g., vertical migration capabilities of the associated organisms. But, few, if any studies concentrated on scattering layers associated with mid-ocean ridges.

*Corresponding author. Department of Biology, University of Bergen, Høyteknologisenteret, Pb 7800, N-5020 Bergen, Norway.
Tel.: +47 55584466; fax: +47 55584450.
E-mail address: anders.opdal@bio.uib.no (A.F. Opdal).

0967-0645/$ - see front matter © 2007 Elsevier Ltd. All rights reserved.
doi:10.1016/j.dsr2.2007.09.002

Therefore, in the wider context of the MAR-ECO study of pelagic nekton and zooplankton diversity (Bergstad and Godø, 2003; Sutton et al., 2008; Gaard et al., 2008), we were interested in exploring the occurrence, distribution and identity of such scattering layers over the Mid-Atlantic Ridge of the North Atlantic. Utilizing the hydroacoustic instrumentation and depth-stratified midwater trawling capability of the R.V. *G.O. Sars*, we hoped to detect and describe scattering layers at full ocean depth in the extensive ridge segment from just south of Iceland to the Azores, but focusing especially on mesopelagic scattering layers.

Our approach was exploratory, in view of the lack of previous area-specific knowledge. The only previous large-scale acoustic studies bordering on our study area were the international redfish (*Sebastes* sp.) surveys that showed enhanced density of backscattering organisms along the Reykjanes Ridge (the segment of the Mid-Atlantic Ridge just south of Iceland) (Sigurdsson et al., 2003). The objective of our study was to describe and collect basic information on pattern, since broad generalities about the functioning of large marine ecosystems are hard to draw from a single, continuous cruise track.

Others have investigated how single and relatively shallow seamounts impinge on DSLs attributed to mesopelagic fish (Genin and Boehlert, 1985; Genin et al., 1988; Rogers, 1994; Fock et al., 2004) and continental slopes (e.g., Mauchline and Gordon, 1991). Isaacs and Schwartzlose (1965) suggested that zooplankton were trapped over the shallow seamounts while undergoing diel vertical migration (DVM). Unable to escape from the plateau when ambient light levels increase, they might become highly visible to predators. Mauchline and Gordon (1991) found a mid-slope maximum in abundance of demersal fishes associated with the daytime depth of mesopelagic scattering layers being concentrated near the seabed along the continental slope. Alternative mechanisms explaining high densities of pelagic macrofauna around seamounts include topographic effects on local hydrographical conditions leading to increased mobilization of new nutrients, enhanced primary productivity and increased densities of prey over seamounts (Genin and Boehlert, 1985; Boehlert and Genin, 1987; Beckmann and Mohn, 2002; Mohn and Beckmann, 2002). However, actual studies at several seamounts worldwide produced contrasting evidence (Rogers, 1994). Neither Martin and Nellen (2004), Schnack and Henning (2004), nor Pusch et al. (2004) found any differences in zooplankton densities above the plateau or above the slope of the Great Meteor Seamount compared to the surrounding oceanic waters. Genin et al. (1988) came to similar conclusions when investigating feeding in epibenthic fish on a shallow bank in the Southern California Bight. Martin and Nellen (2004) observed plankton migrating downwards at dawn over the seamount. They also suggested that observations of low plankton densities above seamounts during night are due to amplified predation in daylight, implying that zooplankton are trapped in shallow waters and preyed upon by visually searching demersal predators during the day. Another explanation for reduced densities at night proposed by Schnack and Henning (2004) is physical displacement of migrating zooplankton during the day when their descent is blocked by the summit. Similarly, Pusch et al. (2004) hypothesized that demersal stocks on the Great Meteor Seamount may be supported by a flow-through energy supply instead of an autochthonous energy source generated by locally enhanced primary production.

Following our description of scattering layers, density patterns and associated environment data on the Mid-Atlantic Ridge, we compare and contrast our findings to the above observations and theories from seamounts and continental slopes.

2. Material and methods

2.1. Sampling strategy in relation to bathymetry

The acoustic studies reported in this paper are based on sampling during Leg 1 of the June–July 2004 expedition on the R.V. *G.O. Sars* (de Lange Wenneck et al., 2008), i.e., the southward voyage from south of Iceland to the Azores. Due to lack of information on the character and distribution of acoustic backscattering patterns prior to the investigation, we chose a systematic zig-zag survey design, ensuring several crossing of the ridge axis and of known physical features such as the Charlie-Gibbs Fracture Zone (CGFZ) and the Sub-polar Front. The objective was not to derive total density estimates for the entire area, but rather to look for large-scale spatial patterns. Acoustic observations were made continuously, and the presentation of results utilizes data from both the entire track of the vessel and three selected cross-ridge transects (Fig. 1).

The three transects represented northern waters of the Reykjanes Ridge, the CGFZ and the southern part of the ridge, respectively (Fig. 1). These transects were used as a basis for describing cross-ridge patterns of acoustic backscattering, in relation to bathymetry and environmental variables, and data on biota from other sources. The bathymetry of the northern transect is best described by a main series of 900–1200 m peaks from ca. 35.5 to 34°W, with a smaller and deeper peak to the east between ca. 32.5 and 32°W (note the use of decimal degrees throughout this paper). The section across the CGFZ bears little resemblance to that in the north, and is characterized by two pronounced deep rift valleys, termed here the western (at 32.25°W) and eastern (at ca. 31.75°W) rift valley, respectively. The southern transect has a single main peak at ca. 29.1°W rising to depth of 1000 m with a nearly 3000 m deep axial valley just to the west of it. Neither of the three transects spanned the entire width of the Mid-Atlantic Ridge into the abyssal plains on either side, and the reason for that was mainly lack of ship-time.

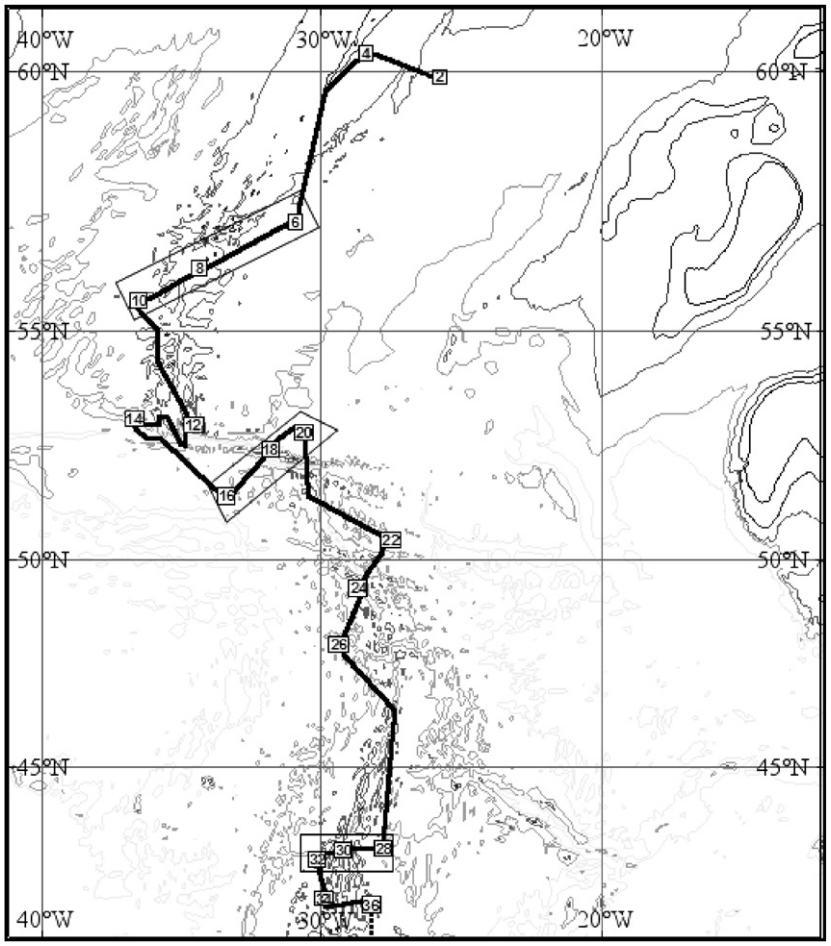

Fig. 1. The track of the vessel, CTD and trawl stations on Leg 1 of the MAR-ECO expedition, 2004. Three main cross-ridge transects analyzed in some detail in the paper are shown as boxes: the northern (Stations 6, 8 and 10), the CGFZ (Stations 16, 18 and 20), and the southern (Stations 28, 30 and 32) transect.

2.2. Acoustic sampling and analysis

The acoustical sampling was performed using a five-frequency (18, 38, 70, 120 and 200 kHz) Simrad EK-60 echosounder, with transducers mounted on a protruding keel 8 m below the surface (see more information in de Lange Wenneck et al., 2008). However, only data collected using the 18-kHz transducer were used in this paper. This frequency yields higher quality echograms from deep water, compared to the more conventional 38 kHz. The 38-kHz echosounder had a noise removed sampling range of 1500 m, compared to 2500 m for 18 kHz. The threshold value, set to −81 dB, significantly reduced the effective sampling range when deep-scattering layers were scarce. Visual comparison of 18 and 38 kHz echograms showed that data were not lost to the 18 kHz compared to 38 kHz. Pulse interval rate was set ">4 s" to allow time for echoes to return from the deepest scatterers and to minimize noise interference with other acoustical instruments. The data permit multi-frequency analysis of the recordings in the upper layers (Korneliussen and Ona, 2002), but this was beyond the scope of this study that targeted large-scale patterns of relatively deep recordings. Furthermore, the sampling intensity was too low to actually validate the acoustic categorization and strong diel processes affecting the frequency response of certain categories, probably due to alteration of the swimbladder properties during ascent and descent.

The Bergen Echo Integrator (BEI) (Foote et al., 1991) was used for post-processing the raw echo sounder data. For each of the 1 nm observation intervals, the raw acoustic data (echograms and associated target strength estimates) were subjectively scrutinized, and assigned observed and adjusted backscattering values (s_A) to the layers 1–6 shown in Fig. 2. Layer 1 had low target strength recordings only, probably attributable to epipelagic mesozooplankton, and the recordings from this layer were confounded by acoustic noise. Layer 6 included near-bottom recordings attributed to benthopelagic organisms, i.e., not the meso- and bathypelagic scatterers targeted in this study. Layers 1 and 6 were therefore excluded from further analysis. All statistical analysis were performed with the SAS software (SAS Institute Inc., 1990).

The weighted depth distribution $\bar{d}_{i,j}$ of each of the six acoustic backscattering layers (i) for each sample (j) (1 nm)

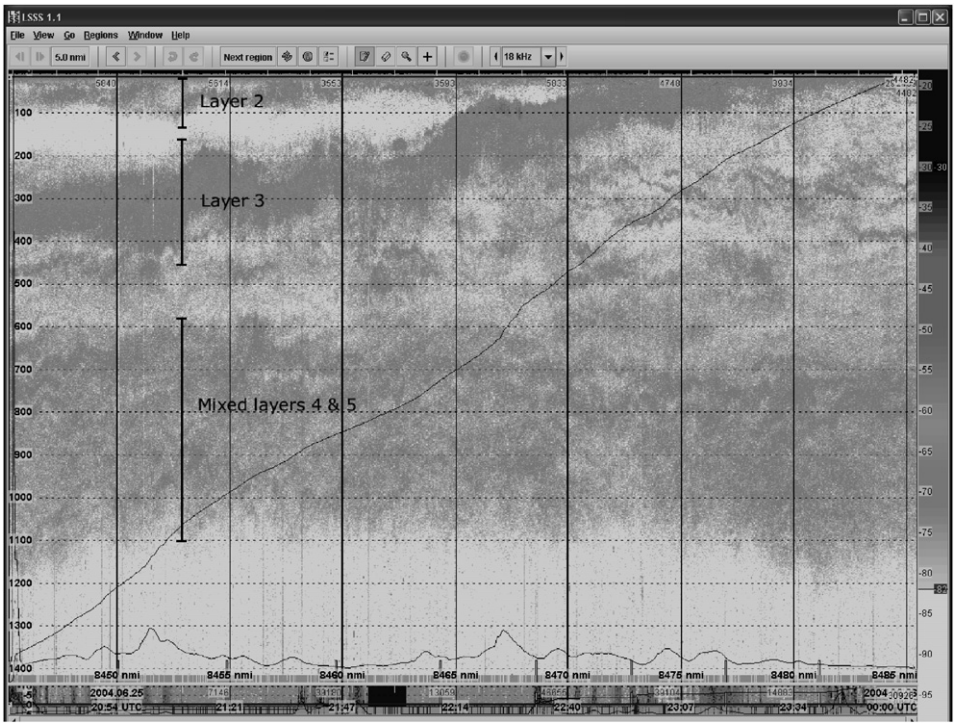

Fig. 2. Echogram from a 40-nautical mile segment recorded between 21:00 h and midnight (local time) illustrating the different layers and their merging during night. The layers 4 and 5 are indistinguishable in this specific echogram. Depth range shown is 0–1400 m, and the seabed at ca. 3500 m is not included.

was calculated as

$$\bar{d}_{i,j} = \frac{\sum_z s_{Ai,j} z_i}{\sum_z s_{Ai,j}}, \quad (1)$$

where s_{Ai} is the recorded mean area backscattering from each discrete depth interval (z_i) each nautical mile (j) of sampling. At night, some of the mesopelagic layers migrated upwards and merged into a single layer (see Fig. 2), but backscattering values were still subjectively assigned according to the original layer definition. A further complication was that layers that were easy to define during the day split into a non-migrating and migrating component during the evening ascent (Fig. 2), rejoining again as a single layer during the descent the following morning.

The result of the post-processing using BEI was a table containing the following data for each nautical mile: latitude, longitude, area backscattering (s_A) for the entire water column, date, time (UTC), maximum and minimum bottom depth, the area backscattering values assigned to each of the six layers and observation depth (d_i) for each layer. Because the total area backscattering varies throughout the day (Engås and Godø, 1986; Aglen, 1994; Michalsen et al., 1996; Stensholt et al., 2002), the acoustic data were analyzed for diel variations using the software application DIVA V2.2.0.4 (Hjellvik, 2005). This software performs a statistical analysis of how a variable (in our case area backscattering) is affected by the time of day. A best fit of either a logistic or sinusoid function is applied to the data, and the fitted function is used to compensate for any systematic day/night differences. We found no significant day/night effects in the total area backscattering (depth-integrated over all layers; 0–1500 m). However, when we studied individual layers, opposite diel trends appeared with increased backscatter in layer 2 and 4, while decreasing in layer 3. No significant day/night variation was found in layer 5.

2.3. Environmental data collection

Data on the abiotic environment was collected continuously along the ship's track and at fixed stations. Details on instruments and procedures are given in de Lange Wenneck et al. (2008) and Søiland et al. (2008). In this study, we utilized the data on currents from the hull-mounted ADCP and the data on near-surface temperature and Chl-*a* derived from fluorescence measurement from the ship's thermosalinograph. In addition, we used data on full ocean depth temperature from CTD casts on every transect, and associated Chl-*a* concentrations from 0–120 m, again derived from fluorescence measurements. Since photosynthesis and fluorescence are dependent on light, systematic diel variation occurred. All Chl-*a* data presented have been adjusted for this variation using the DIVA software. At present there is no documentation on the validity of using logistic functions specifically for Chl-*a* corrections. The diel variation in Chl-*a* can, however, be explained by a logistic function (similar to that of the acoustic backscattering), and may therefore adequately be analyzed by DIVA.

Surface irradiance was recorded continuously (photosynthetically active radiation (PAR) μmol photons/s/m^2) by a Kipp & Zonen PAR LITE sensor for photosynthetic photon flux. Irradiance throughout the cruise varied from about 300 to 2200 μmol photons/s/m^2 at midday.

2.4. Biotic sampling

Meso- and bathypelagic macrofauna was sampled at 16 stations along the ship's track (Fig. 1) using a midwater pelagic fish trawl (Aakra trawl) and a macrozooplankton trawl, both with multiple cod-ends, towed at a speeds of ca. 2 m/s (see further details on gear and procedures in de Lange Wenneck et al. (2008)) in pre-determined depth strata. The maximum and minimum depths sampled in each stratum varied somewhat, and details for individual trawls are given in de Lange Wenneck et al. (2008). The catches were sorted to species, and the resulting biotic database contains numbers and summed weight for individual species. Details on tows and catches were presented by Sutton et al. (2008).

Rough estimates of average weight of an individual in each trawl haul were calculated on the basis of the total number and total weight of the fish catch in each cod-end:

$$\bar{w}_i = \frac{W_s}{N_s}, \quad (2)$$

where $\bar{w}_i$ is the average individual weight of the fish in a sample, W_s is the total weight of fish in the sample (s) and N_s is the total number of fish in the sample (s). To analyze variation in average fish size between depth intervals, a Wilcoxon signed rank sum test (Johnson and Bhattacharyya, 2001) was performed since the size distribution in each depth interval were considered interdependent.

3. Results

3.1. Structure and character of the scattering layers

In good weather and at low vessel speed and using the 18-kHz transducer, layers of sound-scattering organisms could be discerned with certainty to a maximum depth of 3000 m (Fig. 3). This extended the range of observation to all relevant depths observed in the study area with the exception of the very deepest areas of the CGFZ. Multiple meso- and bathypelagic layers of scatterers occurred in the entire area, and also classical diurnal vertical migration of components of these layers (Fig. 2).

Our six-layer categorization was useful for the entire voyage, at least for studying major patterns of distribution and density. We limited our analysis to a maximum depth of 1500 m to avoid unfounded conclusions beyond the secure detection range of the 18-kHz sounder.

3.2. Latitudinal gradients of area backscatter

When plotted along the ship's track, we found large medium-scale variation, but also a large-scale latitudinal pattern in the total acoustic backscattering. The area backscatter from the surface to 1500 m (layers 2–5) is presented over the latitude-gradient in Fig. 4. The highest backscattering, presumably attributable mainly to meso- and bathypelagic fish, occurred just south of the CGFZ from 51 to 46°N. Lower backscattering occurred to the north (>51°N) and south (<46 °N) of this elevated zone.

Both Chl-*a* concentrations and backscattering increased steadily from north towards a maximum around the CGFZ, followed by a decline towards the south (Fig. 5). However, while Chl-*a* concentration dropped to near zero

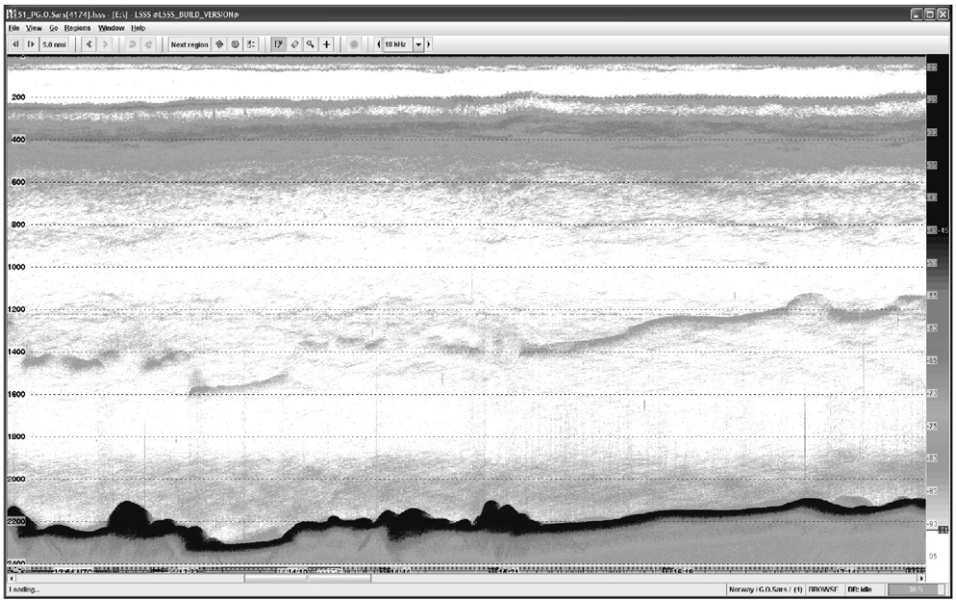

Fig. 3. Echogram from the EK 60 18-kHz echosounder showing pelagic scattering layers from the epipelagic zone to 2400 m.

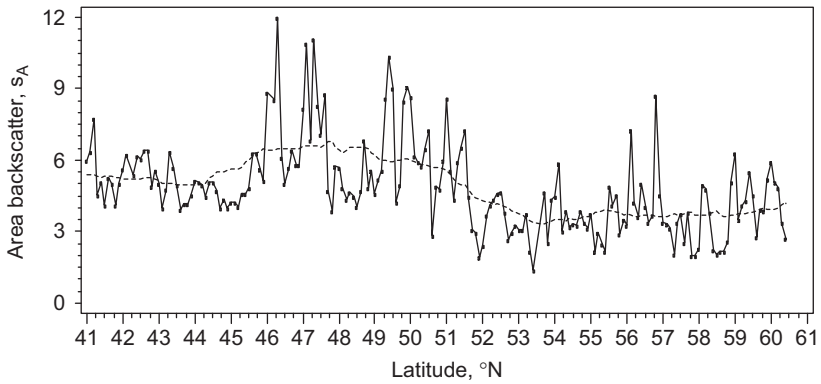

Fig. 4. The mean depth-integrated (0–1500 m) area backscattering, s_A, over 1 nm plotted as a function of latitude to illustrate the north–south gradient of mesopelagic biomass. A 35-point moving average is drawn as a dotted line to illustrate the overall pattern.

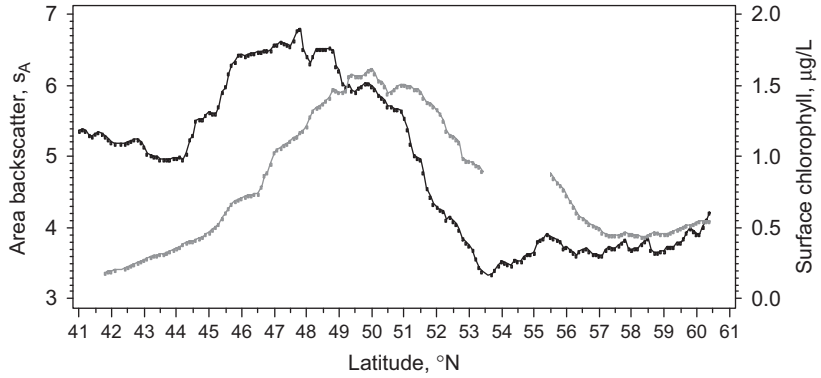

Fig. 5. The latitudinal variation of surface Chl-*a* (grey line) and smoothed mean depth-integrated area backscattering (black line). Due to logging problems, no Chl-*a* observations were recorded between 55.5 and 53.5°N.

in the far south, the area backscattering remained at intermediate levels.

3.3. Longitudinal transects of Chl-a and acoustic densities

In the northern transect (Fig. 6A), an increase in s_A, was observed above the main plateau and the smaller eastern peak. Surface Chl-*a* concentration tended to be higher east of both the main plateau and the smaller eastern peak. In the CGFZ (Fig. 6B), the highest s_A values were present above and between the western and eastern rift valleys. An area of continuous and slightly higher concentrations of Chl-*a* appeared above the two rift valleys. The southern transect (Fig. 6C) had low backscattering immediately above the main peak, followed by a slight increase both to the east and west. Very low concentrations of Chl-*a*, and no systematic variation was observed.

3.4. Fish composition and size structure in the acoustic layers

Attempts were made to determine the taxonomical composition of the scatterers forming layers by examining the catch composition of midwater trawls from the acoustic layer depths, identifying numerically dominant potential sound-scatterers. In the depth-interval considered here, we assumed that the main scatterers were fish. Because the trawl sampling was oblique, sampling through several acoustic layers, and because the layers varied in depth through the day, only rather general and somewhat imprecise information could be derived. Details on the taxonomical composition of the trawls and the meso- and bathypelagic fish distribution are given in Sutton et al. (2008), and the following is mainly based on conclusions drawn in that account.

The abundant and more widespread near-surface fish was the Müller's pearlside (*Maurolicus muelleri*), and it is probable that this species and zooplankton were the main scatterers in the 0–200 m depth zone (layers 2 and 3), at least during the day. The faunal assemblage in the deeper epipelagic and mesopelagic zone southwards towards around 47°N was dominated by the lanternfish *Benthosema glaciale* (Myctophidae), both in numbers and biomass. Further south towards the Azores, the diversity of myctophids increased, and *B. glaciale* was no longer the dominant species. The abundance and biomass in the catches decreased to about half the level observed in the more northern segment of the ridge.

The waters below 750 m were populated by one widespread bathypelagic fish assemblage during the time of this

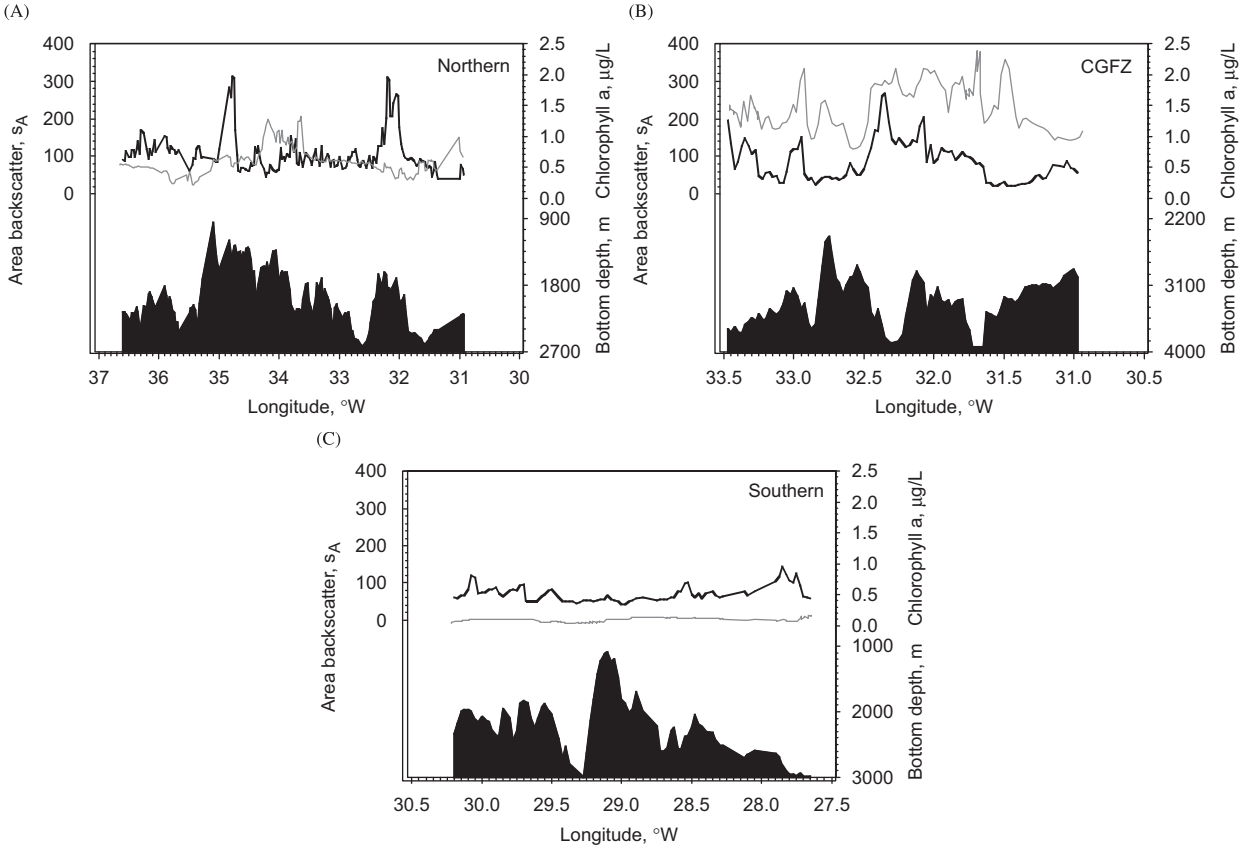

Fig. 6. The concentration of surface Chl-*a* (grey line), and the depth-integrated (0–1500 m) area backscatter (black line) plotted together with the bottom profile in three respective longitudinal transects of the ridge: (A) northern, (B) CGFZ and (C) southern.

survey. The assemblage was characterized by the near-total numerical domination of *Cyclothone microdon*, which contributed 88% of total abundance. Among the 64 other species caught in the quantitative (macrozooplankton trawl) samples from this group, only four contributed more than 1% of total abundance: *Bathylagus euryops* (2.3%), *Scopelogadus beanii* (1.5%), *Sigmops* (*Gonostoma*) *bathyphilum* (1.4%) and *Lampanyctus macdonaldi* (1.1%). The Platytroctidae were also a conspicuous component of the bathypelagic layer, particularly the species *Maulisia microlepis*, which actually dominated the biomass of some individual trawl samples.

Considering abundance in catches and assumed comparatively high target strengths (based on anatomy and size), the likely primary sound-scatterers, were as follows:

- *M. muelleri*—vertical migrator within epi- and upper mesopelagic zone. Likely dominant in layer 2.
- *B. glaciale*—vertical migrator between epi- and mesopelagic zone. Likely dominant in layers 2 and 3.
- *Notoscopelus kroyeri* and *N. bolini*—vertical migrators in mesopelagic and lower epipelagic.
- *L. macdonaldi*—mesopelagic zone migrator.
- *Scopelogadus beanii*—deep non-migrating mesopelagic species. (<1000 m).
- *Serrivomer beanii*—deep non-migrating mesopelagic species (<1000 m).
- *C. microdon*—very abundant meso- and bathypelagic non-migrator (500–2700 m).
- *B. euryops*—abundant weak migrator at bathypelagic depths. (500–1500 m).
- *M. microlepis*—abundant non-migrator in the bathypelagic and lower mesopelagic zone (700–2000 m and perhaps deeper).

There was a significant difference in mean individual fish weight caught in the various layers (Fig. 7). Mean individual weight increased with depth, and using a Wilcoxon signed rank sum test, pairwise comparisons between mean individual weight for hauls in different depth intervals were found to be significantly different in all cases ($p<0.05$).

3.5. Depth distribution and surface irradiance

The weighted depth distribution ($\bar{d}$, see Eq. (1)) of each of the mesopelagic backscattering layers 2–5 along the three different transects (the north, the CGFZ and the south, respectively) showed a striking relationship with surface irradiance (Fig. 8). A classical DVM pattern was observed; ascent at times of decreasing and descent at times of increasing light levels. The northern transect (Fig. 8A) had longer days and shorter nights compared to other transects, and the vertical migration of the layers was

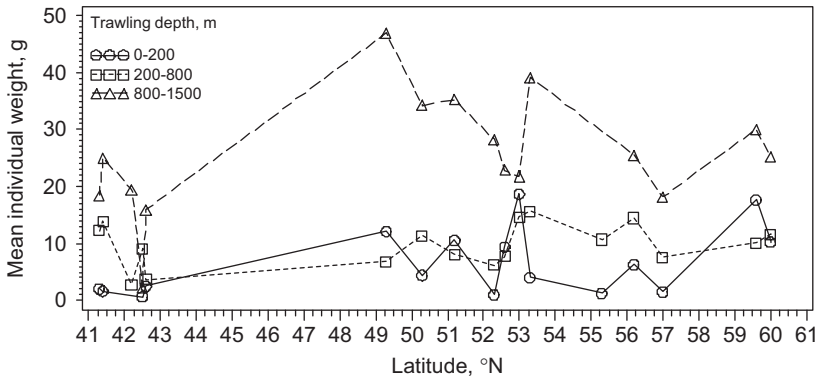

Fig. 7. The average individual fish weight (in grams) in each trawl sample plotted by latitude. Data from the macrozooplankton trawl only.

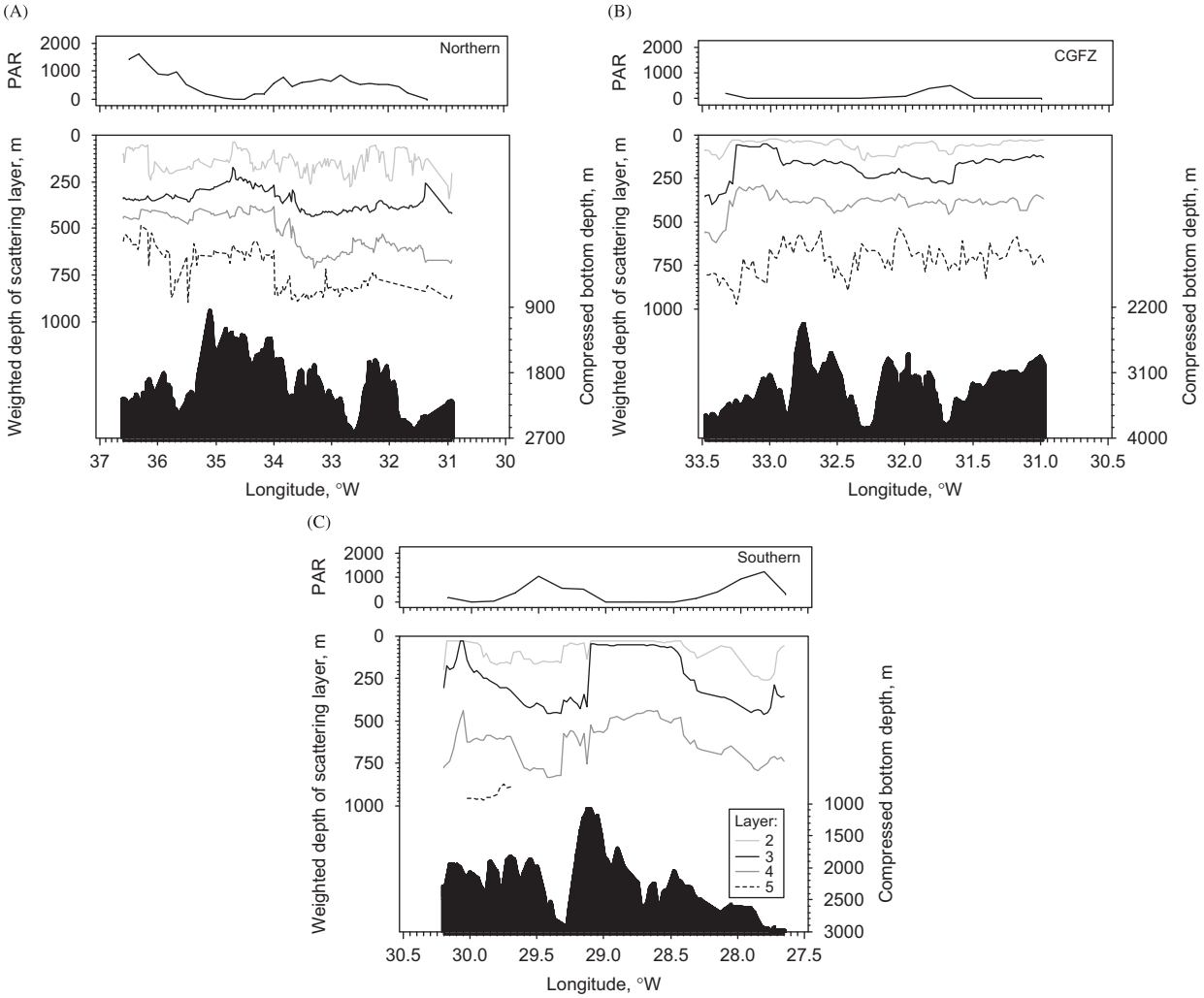

Fig. 8. The weighted depth distribution ($\bar{d}_i$, see Eq. (1)) of the acoustic scattering layers plotted with the bottom profile in three cross-ridge transects of the ridge: (A) northern, (B) CGFZ and (C) southern. The top panels show the photosynthetically active radiation (PAR) on the ship's deck measured as μmol photons/s/m^2.

extensive. The deeper layers (3–5) showed the most pronounced DVM pattern, about 250 m for layer 5 and 100 m for layer 3. In the northern transect, the layers appeared to be shifted deeper on the east side of the main peak compared to the west side. Limited ascent was observed during night at the east end of the transect. In the CGFZ (Fig. 8B), all layers performed a strong ascent during the first night (west side of transect), but did not descend to equivalent depths at dawn (on the east side). In the southern transect (Fig. 8C), a strong DVM was

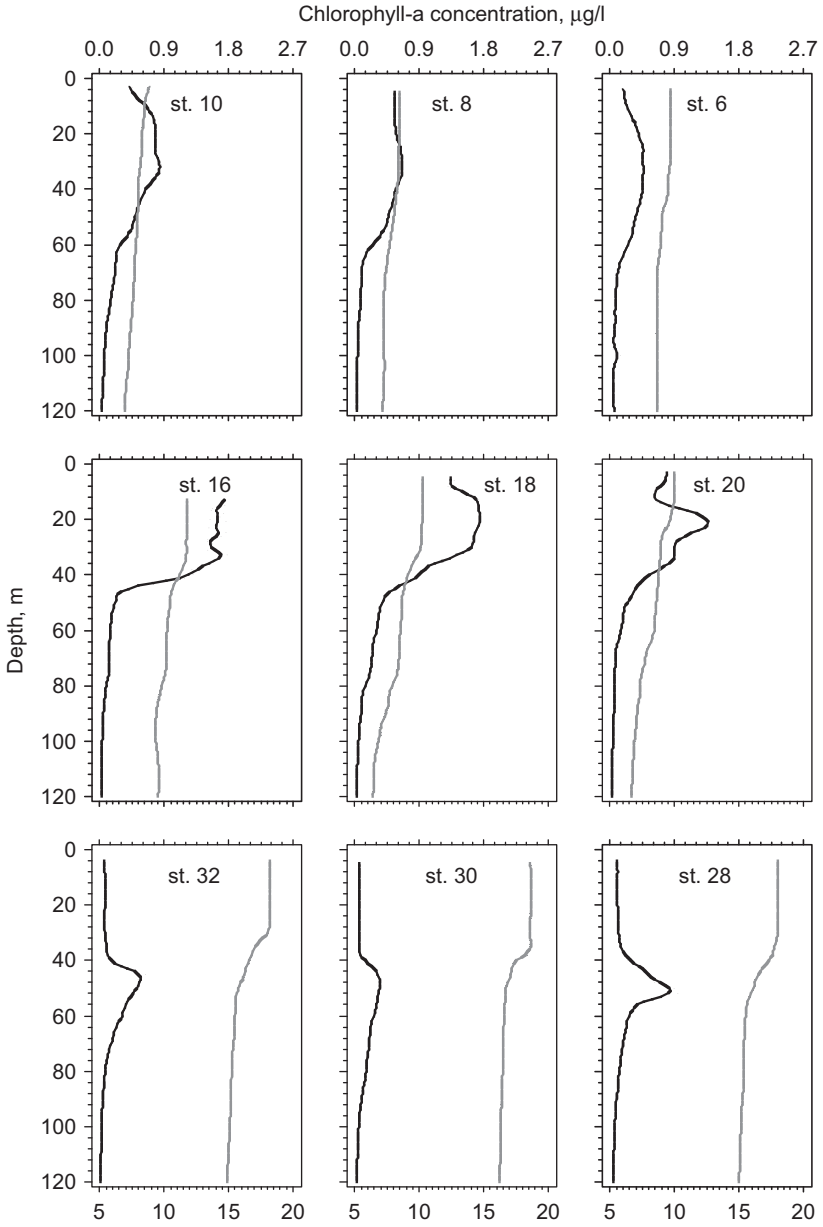

Fig. 9. Chl-*a* (black line) and temperature (grey line) profiles from the nine different stations representing the different cross-ridge transects shown in Fig. 1: northern (CTD-Stations 10, 8 and 6), CGFZ (Stations 16, 18 and 20) and southern (Stations 32, 30 and 28). The horizontal sequence of the plots corresponds to their geographical position, i.e., western on the left, eastern on the right.

observed both nights for all layers, and high irradiance was measured during daytime. Comparing transects, DVM was extensive in the northern and southern zones, and less conspicuous above the CGFZ. Layer 4 (and 5) distributed deeper in the southern transect than in the other two.

3.6. Vertical profiles of Chl-a and physical variables—latitudinal patterns

Nine Chl-*a* and temperature profiles from CTD stations representing three distinct zones of the ridge are shown in Fig. 9. The three southernmost stations (stations 32, 30 and 28) had a distinct deep Chl-*a* maximum layer between 35 and 65 m, with little or no Chl-*a* above or below. There was also a thermocline in the same depth layer. By comparison, the other profiles showed higher concentrations of Chl-*a* at the surface, less distinct Chl-*a* layers and a more gradual decrease in temperature with depth. The highest concentrations of Chl-*a* were found in the CGFZ and in the neighboring areas south of it.

A positive correlation was found between the depth-integrated Chl-*a* concentrations in the upper 200 m, recorded by the CTD, and the co-occurring surface Chl-*a*, derived from the fluorescence measured with the thermosalinograph (Fig. 10). There is a transition in the continuous Chl-*a* recordings on a latitudinal scale (Fig. 11). From moderate levels in the northern areas (61–55°N), increasing to relatively high levels with distinct peaks

between 54 and 46°N, around the CGFZ, and a successive decrease to near-zero levels in the southernmost area of the ridge. The 35-point moving average suggests a maximum concentration of Chl-*a* above the CGFZ at 50°N. The surface temperature decreased slightly from the north to the CGFZ, from where it increased steadily towards the south. These patterns were consistent with the CTD measurements of Chl-*a* and temperature (Fig. 11).

4. Discussion

4.1. Sampling design and methodology

The acoustic mapping was but one element of the multi-disciplinary activity on the MAR-ECO expedition, and with the limited ship-time available, this exploratory study could only produce large-scale pattern information over the huge study area. One constraint was that the transects across the ridge could not be extended very far off the ridge axis, and our results cannot be used to draw firm conclusions on the effects of the ridge as a topographical feature on pelagic scattering layers at an ocean-wide scale.

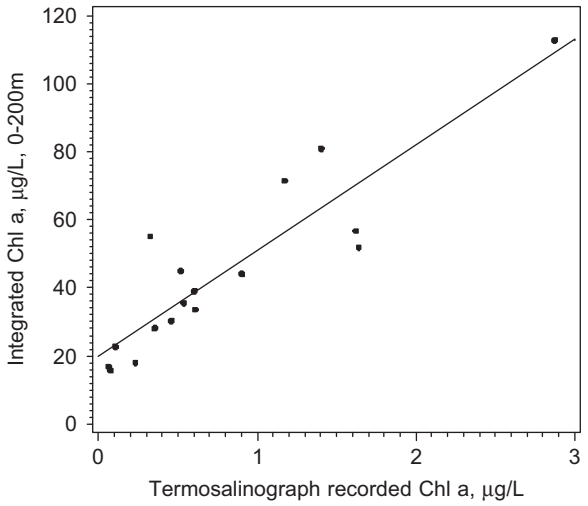

Fig. 10. Regression plot between surface Chl-*a* derived from the thermosalinograph fluorometer and depth-integrated Chl-*a* (0–200 m) measured by fluorometer on the CTD rosette. $R^2 = 0.80$, $p < 0.0001$, S.E. = 3.91 and $n = 17$.

The acoustics facilitated continuous observation of sound-scattering organisms or objects from near-surface waters to great depths, in this case to about 3000 m, over extensive distances. The noise-reduced vessel and the use of the 18-kHz transducer mounted on the drop-keel proved a good solution that extended the observation to virtually all relevant depths. The scale of observation is thus superior to all other methods of sampling, e.g., by optics or fishing gears. However, since the transducer is mounted 8 m below surface and has an additional 3 m of near field, scatterers of the upper 11–12 m are not sampled and are considered to be in the "surface blind zone" (Aglen, 1994; Simmonds and MacLennan, 2005). The combined backscatter of all layers did not reveal any variation between day and night, but echograms from a moored seabed-to-surface directed echosounder (see, e.g., Godø et al., 2005) in the CGFZ show substantial migration into the surface blind zone during night. Similarly, a drifting buoy-mounted echo-sounder with a surface-directed transducer deployed at 20 m in a nearby location confirmed the observation with better resolution (unpublished data, Institute of Marine Research).

Identification of scatterers is not trivial over wide areas and depth ranges, even with a depth-stratifying midwater trawl system as used in this study. Only in a few cases could specific layers be targeted, and as a rule the tows were oblique through constant depth intervals of several hundreds of meters. Single acoustic layers typically occupied much narrower and varying depth intervals and trawl catches therefore seldom represented a well-defined acoustic layer. We, therefore, had to rely on a general account of the trawl catches and fish assemblages by Sutton et al. (2008) to determine what fish species were probably the main organisms creating our echogram patterns. Furthermore, small abundant species such as *Cyclothone* may have been under-sampled due to their small size (Pusch et al., 2004; Sutton et al., 2008).

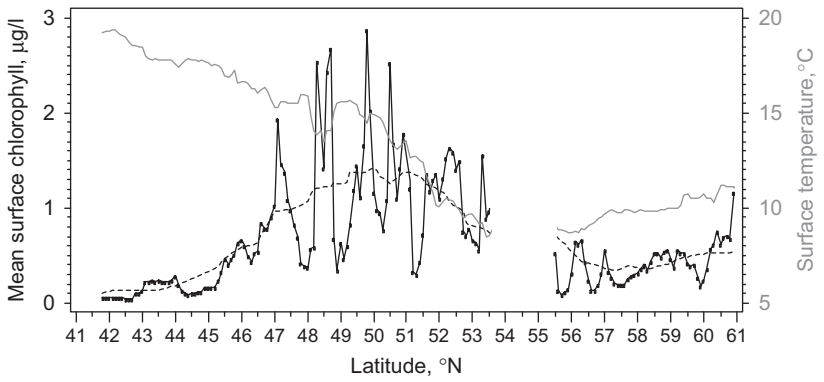

Fig. 11. The variation of mean surface chlorophyll-a concentrations of 1 nm derived from the thermosalinograph fluorometer plotted by latitude (black line). The dotted line is a 35-point moving average of the summed layer 2–5 area backscatter. Surface temperature from the thermosalinograph is shown in grey. Due to logging problems, no observations were recorded between 55.5 and 53.5°N.

It is generally believed that more biomass in mesopelagic water masses is recorded by the echosounder than is captured in trawl samples (Wardle, 1993). This implies that all recorded backscattering cannot be simply attributed to the fish or plankton caught in trawl samples. The echosounder recordings may include various organic aggregates with trapped air bubbles not sampled by the trawls. However, the error created by this effect cannot readily be quantified.

In accordance with other acoustic studies on migration of mesopelagic fish in other waters (Clark and Levy, 1988; Giske et al., 1990; Rosland and Giske, 1994; Kaartvedt et al., 1996), we also found significant merging of layers during the night. An increase in s_A in layer 3 and corresponding decrease in layers 2 and 4 at night suggests inconsistency in the interpretation and merging of layers. Systematic changes in fish tilt angle between night and day are also known to cause variation in area backscatter (Aglen, 1994). Tilt angle is also found to vary with depth (Huse and Ona, 1996) and is influenced by vessel avoidance (Olsen et al., 1983a, b). The recordings never reached levels where shadowing (Aglen, 1994; Simmonds and MacLennan, 2005) started to affect results. A varying effect of resonance in swimbladdered fish (Aglen, 1994; Simmonds and MacLennan, 2005) of this size is expected at 18 kHz during DVM and this could, for example, compensate for losses of fish migrating into the surface blind zone. Such effects are difficult to assess and predict based on the limited knowledge of the actual acoustic target strength of mesopelagic fish. Fish species containing gas-filled swimbladders will also give higher area backscattering than species with lipid-filled bladders or species without this organ. These problems may confuse comparisons between acoustics and trawling.

4.2. Along-ridge patterns

A main pattern observed was the maximum in backscattering in the area just south of the CGFZ, presumably reflecting a maximum zone in the density of meso- and bathypelagic fish. The density appeared substantially lower to the north and south of this zone, but surprisingly higher in the south than in the north. The pattern is the opposite for density estimated from midwater trawls (Sutton et al., 2008).

The apparently high concentrations of Chl-*a* above the CGFZ coincide with the front between the Sub-polar and the Sub-tropical Gyres (Søiland et al., 2008). The depth profiles at and just south of the CGFZ showed relatively high concentrations of Chl-*a* down to 50–70 m. We did not have access to productivity measurements, and we cannot conclude that there is a positive correlation between primary production and standing stock of any taxa observed. However, it is likely that primary productivity, including mesopelagic communities, differ between northern and southern areas and are related to the dominating surface currents and watermass characteristics. While nutrient-rich cold water from the Sub-polar Gyre supplies the northern areas, the comparatively nutrient-depleted warm North Atlantic Drift and the watermasses of the Sub-tropical Gyre dominate in the south (Søiland et al., 2008). The Sub-polar Front was apparent during the survey as an abrupt change in surface temperature around and just south of the CGFZ. Richardson and Schoeman (2004) reported a similar division between turbulent-nutrient-rich cool waters in the northern part, and stratified-nutrient-poor warm waters in the southern part of the North Atlantic. Analogous temperature-related regimes were described by Bouman et al. (2003). The low phytoplankton abundance in the south is likely to be a permanent condition, as the satellite images of this ridge segment show little or no Chl-*a* in that area throughout the year. Continuous high temperatures in the southern region are believed to promote strong stratification (Roemmich and McGowan, 1995), diminishing potential nutrient supplies from deeper waters.

4.3. Cross-ridge gradients

In the northern transect, an increase in area backscattering occurred very near the two maxima of surface Chl-*a* concentration that occurred above and slightly to the east of the two topographical peaks. This pattern is similar to that explained as a productivity maximum created by upwelling of cold nutrient-rich water at the Minami-kasuga Seamount in the northwest Pacific (Genin and Boehlert, 1985). The relatively strong (tidal) current directly above the shallow areas of the transect may generate mixing of water masses (Genin et al., 1989; Søiland et al., 2008). A rise in phytoplankton surrounding the northern ridge segment summit would be a pattern in accordance with the often-expressed view that sub-marine structures provide a favorable habitat for marine life (Genin and Boehlert, 1985; Genin et al., 1989; Rogers, 1994; Fock et al., 2004), but our data are too sparse and geographically and temporally limited to reach a firm conclusion.

A similar match between phytoplankton and mesopelagic scattering was not found in the southern transect. Near-zero levels of acoustic backscattering directly above the ridge may reflect a weaker and different relationship to that found in the north. The biotic sampling confirms differences between north and south in species composition (Sutton et al., 2008), but trophic patterns are not well studied.

In the CGFZ, area backscattering and concentration of surface Chl-*a* above the two rift valleys seemed to coincide. The front of warm and cold watermasses may provide strong mixing and good conditions for phytoplankton production and pelagic biota, relatively independent of bathymetric features in this deep area.

4.4. Size structure and vertical distribution

The successive increase in average individual weight with increasing depth is in accordance with earlier studies on

size distribution of fish and zooplankton in vertically structured backscattering layers (Giske and Aksnes, 1992; Torgersen and Kaartvedt, 2001). It seems reasonable to assume that the acoustic layers will exhibit similar depth-related size distribution patterns as those observed in the depth-stratified catches.

The diel dynamics of mesopelagic organisms has been studied extensively (Clark and Levy, 1988; Kaartvedt et al., 1996; Pearre, 2003), and is believed to be a behavioural response to foraging success and mortality risks under changing light intensities. We observed the classical upward and downward migration in the water column with decreasing or increasing light intensities. Several studies have found that mesopelagic fish respond instantaneously to slight changes in light intensity (Giske et al., 1990; Baliño and Aksnes, 1993). Throughout all transects, layer 2 seemed to be the least dynamic with regards to DVM. From the calculations of mean individual weight in the biotic samples, this layer seems to consist of smaller individuals than the deeper layers.

We observed a deeper average vertical distribution in the eastern than in the western part of the northern transect. The corresponding light levels were lower in the east than in the west during daytime, thus it is unlikely that this difference is light driven. Chl-*a* is an important contributor to light attenuation, and is known to cause shallower distribution of sound-scattering layers (e.g., Kaartvedt et al., 1996). We did not, however, find any significant differences in Chl-*a* concentrations between east and west. Temperature recordings from the CTD stations show that the water temperature on the eastern side is ca. 1 °C warmer than in the west. However, it is difficult to see how this rather slight temperature difference could explain differences in vertical distribution.

The depth range of DVM differed between transects. We suggest that low Chl-*a* concentrations in the southern transect and the associated lower light attenuation and stronger day/night differences in light-at-depth results in more intense vertical migration in the southern transect. This interpretation is consistent with other studies on vertical distribution of sound-scattering layers and Chl-*a* (Kaartvedt et al., 1996; Aksnes et al., 2004; Aksnes, 2007).

4.5. Conclusions and hypotheses

We observed widespread and usually layered meso- and bathypelagic backscattering along and across the Mid-Atlantic Ridge in our study area, and we were able to detect scatterers to a depth of about 3000 m. We observed a pronounced maximum in backscattering, and presumably fish density, in the area associated with the Sub-polar Front near and just south of the CGFZ. The overall latitudinal pattern suggested transitions between three different zones: the Reykjanes Ridge, the Sub-polar Front and the subtropical zone southwards towards the Azores. Cross-ridge variation and patterns were most pronounced in the two northern zones.

Given the pronounced variability in temperature, depth and presumed epipelagic production, there may be several different driving forces which explain the observed patterns of distribution of scattering layers along and across the ridge. One feature of the ridge system is the apparent absence of epipelagic schooling planktivorous fishes. Although neither methods sample the surface waters well, both the trawl samples and echograms revealed no such species. If this is correct, it suggests that the epipelagic production mainly fuels a mesopelagic food-web. Primary productivity is influenced by the large-scale circulation system and, to some degree, by the bottom topography. We found an interesting latitudinal gradient in Chl-*a* concentrations and area backscattering levels, and although the relationship is weak and explicit evidence lacking, it is tempting to suggest that this reflects differences in productivity patterns and a bottom-up regulation of fish abundance. The area north of 53°N is characterized by having moderate concentrations of Chl-*a* and backscattering, and we hypothesize that in this zone the low primary production limits fish abundance. Around the CGFZ (ca. 53–46°N) presence of phytoplankton is significantly higher than in the north, and supports what appears to be higher standing stocks of fish. These two northern regions may therefore be controlled bottom-up, where mesopelagic biomass is dependent on the production of lower trophic levels through enhanced nutrient supply. Whether the phytoplankton production in the north and in CGFZ is sustained by autochthonous nutrients or is simply advective production from oceanic waters crossing the ridge is not clear. However, a major structure such as the Mid-Atlantic Ridge is likely to cause upwelling from crossing currents, fronts and mixing from tidal currents, all of which in turn would bring potentially nutrient-rich water to the surface (Mohn and Beckmann, 2002). Similarly, we hypothesize that the relatively high densities of fish and low concentrations of Chl-*a* in the southern area reflects the view that little new production takes place in this zone. Here, the fish biomass may be sustained by zooplankton advected over the ridge, not dependent on autochthonous nutrient and/or phytoplankton production (Isaacs and Schwartzlose, 1965; Rogers, 1994).

Acknowledgments

We are grateful to Henrik Søiland for discussions and presentations of data on hydrography and currents, to Tracey Sutton and other fish biologists for first-hand information on fish distributions, and to Stein Kaartvedt for valuable comments to earlier drafts of the manuscript. This study was as an element of the MAR-ECO project, a field project of the Census of Marine Life program (www.coml.org).

References

Aglen, A., 1994. Sources of errors in acoustic estimation of fish abundance. In: Fernø, A., Olsen, S. (Eds.), Marine Fish Behaviour

in Capture and Abundance Estimation. Fishing News Books, Bergen, pp. 107–133.
Aksnes, D.L., 2007. Evidence for visual constraints in large marine fish stocks. Limnology and Oceanography 52 (1), 198–203.
Aksnes, D.L., Nejstgaard, J., Sædberg, E., Sørnes, T., 2004. Optical control of fish and zooplankton populations. Limnology and Oceanography 49 (1), 233–238.
Baliño, B.M., Aksnes, D.L., 1993. Winter distribution and migration of the sound-scattering layers, zooplankton and micronekton in Masfjorden, western Norway. Marine Ecology Progress Series 102 (1/2), 35–50.
Beckmann, A., Mohn, C., 2002. The upper ocean circulation at Great Meteor Seamount. Part 2: Retention potential of the seamount induced circulation. Oceans Dynamics 52, 194–204.
Bergstad, O.A., Godø, O.R., 2003. The pilot project "Patterns and processes of the ecosystems of the northern Mid-Atlantic": aims, strategy and status. Oceanologica Acta 25 (5), 219–226.
Boehlert, G.W., Genin, A., 1987. A review of the effects of seamounts on biological processes. In: Keating, B.H., Fryer, P., Batiza, R., Boehlert, G.W. (Eds.), Seamounts, Islands and Atolls. Geophysical Monograph, vol. 43. American Geophysical Union, Washington, pp. 319–334.
Bouman, H.A., Platt, T., Sathyendranath, S., Li, W.K.W., Stuart, V., Fuentes-Yaco, C., Maass, H., Horne, E.P.W., Ulloa, O., Lutz, V., Kyewalyanga, M., 2003. Temperature as indicator of optical properties and community structure of marine phytoplankton: implications for remote sensing. Marine Ecology Progress Series 258, 19–30.
Clark, C.W., Levy, D.A., 1988. Diel vertical migration by juvenile sockeye salmon and the antipredation window. American Naturalist 131, 271–290.
de Lange Wenneck, T., Falkenhaug, T., Bergstad, O.A., 2008. Strategies, methods, and technologies adopted on the R.V. *G.O. Sars* MAR-ECO expedition to the Mid-Atlantic Ridge in 2004. Deep-Sea Research II, this issue [doi:10.1016/j.dsr2.2007.09.017].
Engås, A., Godø, O.R., 1986. Influence of trawl geometry and vertical distribution of fish on sampling with bottom trawl. Journal of Northwest Atlantic Fishery Science 7 (1), 35–42.
Fock, H.O., Pusch, C., Ehrich, S., 2004. Structure of deep-sea pelagic fish assemblages in relation to the Mid-Atlantic Ridge (45°–50°N). Deep-Sea Research Part I—Oceanographic Research Papers 51 (1), 953–978.
Foote, K.G., Knudsen, H.P., Korneliussen, R.J., Nordbø, P.E., Røang, K., 1991. Postprocessing system for echo sounder data. The Journal of the Acoustical Society of America 90 (1), 37–47.
Gaard, E., Gislason, A., Falkenhaug, T., Søiland, H., Musaeva, E., Vereshchaka, A., Vinogradov, G., 2008. Horizontal and vertical copepod distribution and abundance on the Mid-Atlantic Ridge in June 2004. Deep-Sea Research Part II, this issue [doi:10.1016/j.dsr2.2007.09.012].
Genin, A., Boehlert, G.W., 1985. Dynamics of temperature and chlorophyll structures above a seamount—an oceanic experiment. Journal of Marine Research 43 (4), 907–924.
Genin, A., Haury, L., Greenblatt, P., 1988. Interactions of migrating zooplankton with shallow topography: predation by rockfishes and intensification of patchiness. Deep-Sea Research Part A—Oceanographic Research Papers 35 (2), 151–175.
Genin, A., Noble, M., Lonsdale, P.F., 1989. Tidal currents and anticyclonic motions on 2 North-Pacific seamounts. Deep-Sea Research Part A—Oceanographic Research Papers 36 (12), 1803–1815.
Giske, J., Aksnes, D.L., 1992. Ontogeny, season and trade-offs: vertical distribution of the mesopelagic fish *Maurolicus muelleri*. Sarsia 77 w(3/4), 253–261.
Giske, J., Aksnes, D.L., Baliño, B.M., Kaartvedt, S., Lie, U., Nordeide, J.T., Salvanes, A.G.V., Wakili, S.M., Aadnesen, A., 1990. Vertical distribution and trophic interactions of zooplankton and fish in Masfjorden, Norway. Sarsia 75 (1), 65–81.
Godø, O.R., Patel, R., Torkelsen, T., Vagle, S., 2005. Observatory technology in fish resources monitoring. In: Proceedings of the International Conference "Underwater Acoustic Measurements," Heraklion, Crete, Greece, pp. 363–372.
Hjellvik, V., 2005. DIVA 2.2.0.5. Institute of Marine Research, Bergen. ⟨http://www.imr.no/aktiviteter/forskningsgrupper/observasjonsmetodikk/projects/diva⟩.
Huse, I., Ona, E., 1996. Tilt angle distribution and swimming speed of overwintering Norwegian spring-spawning herring. ICES Journal of Marine Science 53, 863–873.
Isaacs, J.D., Schwartzlose, R.A., 1965. Migrant sound scatterers: interactions with the sea floor. Science 150, 1810–1830.
Johnson, R.A., Bhattacharyya, G.K., 2001. Statistics: Principles and Methods, Vol. 4. Wiley, pp. 643–646.
Kaartvedt, S., Melle, W., Knutsen, T., Skjoldal, H.R., 1996. Vertical distribution of fish and krill beneath water of varying optical properties. Marine Ecology Progress Series 136, 51–58.
Korneliussen, R.J., Ona, E., 2002. An operational system for processing and visualizing multi-frequency acoustic data. ICES Journal of Marine Science 59 (2), 291–313.
Martin, B., Nellen, W., 2004. Composition and distribution of zooplankton at the Great Meteor Seamount, subtropical North-east Atlantic. Archive of Fishery and Marine Research 51 (1–3), 89–100.
Mauchline, J., Gordon, J.D.M., 1991. Oceanic pelagic prey of benthopelagic fish in the benthic boundary layer of a marginal oceanic region. Marine Ecology Progress Series 74, 109–115.
Michalsen, K., Godø, O.R., Fernø, A., 1996. Diel variation in the catchability of gadoids and its influence on the reliability of the abundance indices. ICES Journal of Marine Science 53 (2), 389–395.
Mohn, C., Beckmann, A., 2002. The upper ocean circulation at Great Meteor Seamount. Part 1: Structure of density and flow fields. Oceans Dynamics 52, 179–193.
Olsen, K., Angell, J., Løvik, A., 1983a. Quantitative estimation of the influence of fish behaviour on acoustically determined fish abundance. FAO Fish Report 300, 139–149.
Olsen, K., Angell, J., Pettersen, F., Løvik, A., 1983b. Observed fish reactions to a surveying vessel with special reference to herring, cod, capelin and polar cod. FAO Fish Report 300, 131–138.
Pearre, S., 2003. Eat and run? The hunger/satiation hypothesis in vertical migration: history, evidence and consequences. Biological Reviews 78 (1), 1–79.
Pusch, C., Beckmann, A., Porteiro, F.M., Westernhagen, H.V., 2004. The influence of seamounts on mesopelagic fish communities. Archive of Fishery and Marine Research 51 (1–3), 165–186.
Richardson, A.J., Schoeman, D.S., 2004. Climate impact on plankton ecosystems in the Northeast Atlantic. Science 305 (5690), 1609–1612.
Roemmich, D., McGowan, J., 1995. Climatic warming and the decline of zooplankton in the California Current. Science 267 (5202), 1324–1326.
Rogers, A.D., 1994. The biology of seamounts. Advances in Marine Biology 30, 305–350.
Rosland, R., Giske, J., 1994. A dynamic optimization model of the diel vertical migration of a pelagic planktivorous fish. Progress in Oceanography 34, 1–43.
SAS Institute Inc., 1990. SAS/STAT User's Guide: Statistics. SAS Institute Inc.
Schnack, S.B., Henning, S., 2004. Occurrence and distribution pattern of mesozooplankton at the Great Meteor Seamount (subtropical Atlantic). Archive of Fishery and Marine Research 51 (1–3), 101–114.
Sigurdsson, Th., Jónsson, G., Pálsson, J., 2003. Deep scattering layer over Reykjanes Ridge and in the Irminger Sea. ICES CM 2002/M:09, 7.
Simmonds, J., MacLennan, D., 2005. Fisheries Acoustics—Theory and Practice. Blackwell Publishing, Oxford.
Søiland, H., Budgell, W.P., Knutsen, Ø., 2008. The physical oceanographic conditions along the Mid-Atlantic Ridge north of the Azores in June–July 2004. Deep-Sea Research II, this issue [doi:10.1016/j.dsr2.2007.09.015].
Stensholt, B.K., Aglen, A., Mehl, S., Stensholt, E., 2002. Vertical density distributions of fish: a balance between environmental and physiological limitation. ICES Journal of Marine Science 59 (4), 679–710.

Sutton, T.T., Porteiro, F.M., Heino, M., Byrkjedal, I., Langhelle, G., Anderson, C.I.H., Horne, J., Søiland, H., Falkenhaug, T., Godø, O.R., Bergstad, O.A., 2008. Vertical structure, biomass and topographic association of deep-pelagic fishes in relation to a mid-ocean ridge system. Deep-Sea Research II, this issue [doi:10.1016/j.dsr2.2007.09.013].

Torgersen, T., Kaartvedt, S., 2001. In situ swimming behaviour of individual mesopelagic fish studied by split-beam echo target tracking. ICES Journal of Marine Science 58 (1), 346–354.

Wardle, C.S., 1993. Fish behaviour and fishing gear. In: Pitcher, T.J. (Ed.), Behaviour in Teleost Fishes. Chapman & Hall, London, pp. 609–643.